R-01-16

# PARTRACK

## – A particle tracking algorithm for transport and dispersion of solutes in a sparsely fractured rock

Urban Svensson
Computer-aided Fluid Engineering AB

April 2001

**Svensk Kärnbränslehantering AB**
Swedish Nuclear Fuel
and Waste Management Co
Box 5864
SE-102 40 Stockholm Sweden
Tel 08-459 84 00
+46 8 459 84 00
Fax 08-661 57 19
+46 8 661 57 19



SKB

ISSN 1402-3091
SKB Rapport R-01-16

# PARTRACK

## – A particle tracking algorithm for transport and dispersion of solutes in a sparsely fractured rock

Urban Svensson
Computer-aided Fluid Engineering AB

April 2001

# Abstract

A particle tracking algorithm, PARTRACK, that simulates transport and dispersion of solutes in a sparsely fractured rock is described. The main novel feature of the algorithm is the introduction of multiple particle states. It is demonstrated that the introduction of this feature allows for the simultaneous simulation of Taylor dispersion, sorption and matrix diffusion.

A number of test cases are used to verify and demonstrate the features of PARTRACK. It is shown that PARTRACK can simulate the following processes, believed to be important for the problem addressed: the split up of a tracer cloud at a fracture intersection, channelling in a fracture plane, Taylor dispersion and matrix diffusion and sorption.

From the results of the test cases, it is concluded that PARTRACK is an adequate framework for simulation of transport and dispersion of a solute in a sparsely fractured rock.

# Abstract (Swedish)

PARTRACK är en algoritm för simulering av ett ämnes transport och spridning i sprickigt berg. PARTRACK utgår ifrån att en partikels rörelse kan beskrivas med hjälp av ett antal tillstånd, som partikeln kan befinna sig i. Det visas i rapporten att denna metodik gör det möjligt att behandla flera dispersionsmekanismer som verkar parallellt.

Genom en serie testfall visas att PARTRACK ger korrekta resultat. Följande dispersionsmekanismer behandlas i testfallen: Uppdelning i sprickkorsningar, kanalbildning i sprickplanet, Taylor dispersion, matrisdiffusion och sorption.

Från de erhållna resultaten framgår att PARTRACK är ett lämpligt och kraftfullt beräkningsprogram för simulering av transport och dispersion i sprickigt berg.

PLEASE BE AWARE THAT
ALL OF THE MISSING PAGES IN THIS DOCUMENT
WERE ORIGINALLY BLANK

# Contents

# 1 Introduction

## 1.1 Background

Transport of matter from expected repository depth to ground level is for obvious reasons a key issue in performance assessment studies. One presently investigated alternative is to place the repository at a depth of about 500 metres in a crystalline rock without major fracture zones. Radionuclides from field canisters thus have to be transported through a low permeability volume, without major fracture zones, and after that through a system of larger fracture zones.

In this report a computer code, called PARTRACK, which is intended to solve the transport problem described above is presented. No real world applications will however be performed, instead the report focuses on basic verification and demonstration cases.

The model to be described is based on earlier studies within the Äspö Hard Rock Laboratory (HRL) project, see Svensson (1992, 1994). It is a particle tracking algorithm specifically designed for transport and dispersion of solutes in a fractured media. It considers the splitting up of a tracer cloud in fracture crossings and simulates mass transfer and dispersion by postulating that a particle can be in different states. The transition from one state to the other is governed by frequencies, which give the likelihood that a particle will change state during a specified time interval. It is clear that this formalism fits the description of sorption on the surfaces of a flow channel, but it has also been demonstrated, see Svensson (1994), that Taylor dispersion can be described with two states. Simultaneous processes, for example Taylor dispersion and sorption, can however not be described by only two states. The present study aims to eliminating this limitation by introducing an arbitrary number of particle states.

An interesting line of development, that fits in well with the model to be presented, is the multi-rate mass transfer model described in Haggerty and Gorelick (1995). This model allows for small-scale variation in rates and types of mass transfer by using a series of first-order equations to represent each of the mass transfer processes. In the present study we will try to represent the multi-rate mass transfer by the particle states discussed above.

The transport and dispersion processes are strongly linked to the flow field; a good characterisation of the flow paths and pore-velocities is a prerequisite for transport simulations. The particle tracking algorithm to be presented builds upon the flow model presented in Svensson (1999a, b). This is a stochastic continuum model with a conductivity field generated from a fracture network. It is believed that the novel method for generating the conductivity field will prove valuable also when transport simulations are attempted.

A brief review of transport models can be found in Cvetkovic et al. (1999) and the multi-rate transfer model is described in Haggerty and Gorelick (1995, 1998) and McKenna (1999). A general account of flow and transport of solutes in a fractured rock is given by Bear et al. (1993), see also Sahimi (1995).

## 1.2 Objective

The main objective of this study can be stated as follows:

- Demonstrate that the particle tracking algorithm PARTRACK is an adequate framework for simulating transport and dispersion of a solute in a sparsely fractured rock.

In particular we want to verify and demonstrate the following aspects of PARTRACK.

- Show that the introduction of multiple particle states allows for simulation of several processes working in parallel.

- Demonstrate that diffusion into microfissures and pores can be represented by the multi-rate mass transfer model, as introduced in PARTRACK.

- Show that PARTRACK can be coupled with the flow model.

# 2 Basic conceptual assumptions

## 2.1 Introduction

Dispersion can in a general sense be defined as (Abelin et al., 1991) "the broadening of the residence time distribution of a species transported by a fluid as the fluid moves in a medium". There are several possible causes of dispersion like velocity variations, interaction with the rock, etc. These processes will now be discussed, first from a physical point of view and then their representation in a numerical model.

## 2.2 The situation considered

Transport of a tracer travelling through a fracture network leads to dispersion for (at least) the following reasons (see Figure 2-1):

- **Intersections.** At a fracture intersection a tracer cloud may split up and enter pathways with different lengths and fluid velocities. This type of dispersion is often called macro-dispersion.

- **Channelling.** Spreading occurs within each fracture plane as the different streamlines have different path lengths and velocities. The flow channels may also merge or split up.

- **Taylor dispersion.** A velocity profile exists between the two bounding walls of the fracture. The resulting dispersion effect is called shear- or Taylor dispersion.

- **Matrix diffusion and sorption.** Interaction with the rock, stagnant pools and microfissures causes a number of processes that in effect lead to a delay and dispersion of a tracer pulse. These include: sorption on the fracture walls, diffusion into the rock matrix with sorption on inner surfaces and interaction with gauge.

A fairly complete account of contaminant transport in a fractured rock can be found in Bear et al. (1993).

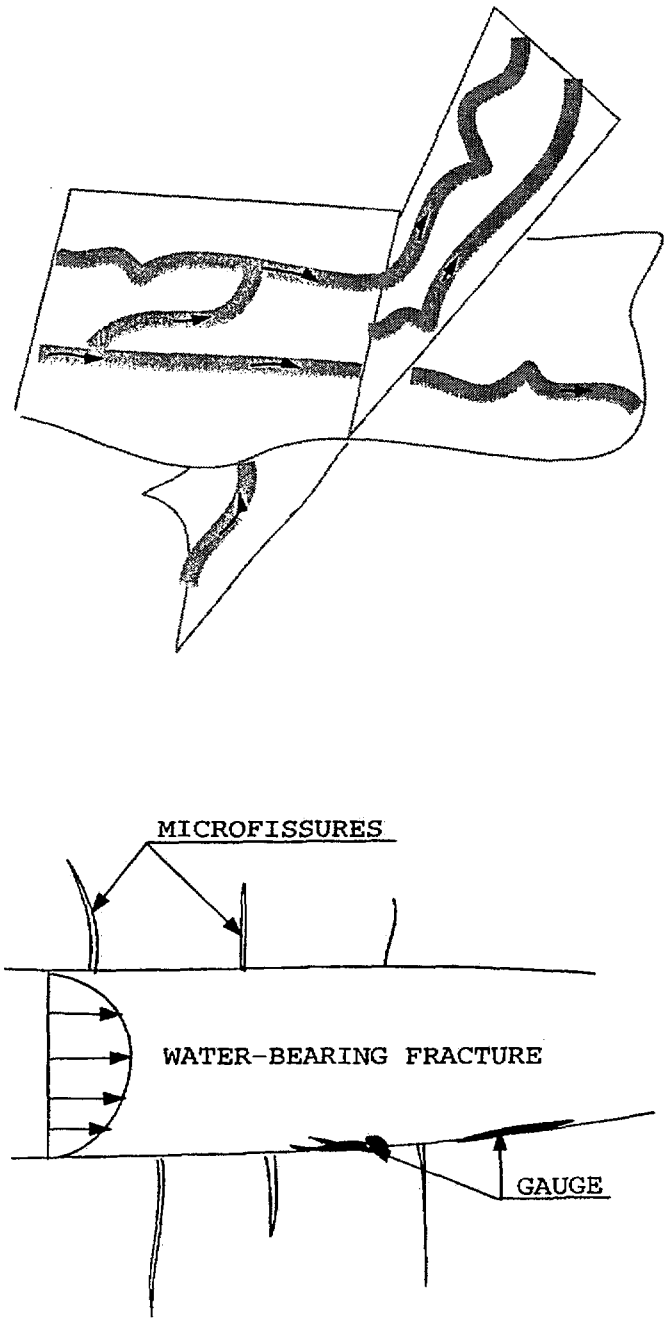


***Figure 2-1.*** *Illustration of processes leading to dispersion of a tracer pulse. Two intersecting fracture planes (top) and micro-scale processes.*

## 2.3 Representation in a numerical model

Before we discuss transport and dispersion a few features of the flow model need to be introduced, as PARTRACK is closely integrated with the flow model. The computational domain is subdivided into control volumes, or cells, which each has a pressure value representing the cell (and other scalars like salinity) and a flow vector associated to each cell wall, see Figure 2-2. The flow is determined from Darcy's law, using the cell pressures and the conductivity representing the velocity control volume. The conductivity fields are calculated from a fracture network, see Svensson (1999a, b). Also the kinematic porosity for the scalar cell is determined from the fracture network as each fracture has a porosity value associated with it. A detailed account of how the fracture porosity is represented as open, or free, volumes in scalar cells is given in Svensson (2001).

The basic idea of PARTRACK can now be described, see also Figure 2-2, as follows:

- A particle entering a scalar cell will, if no dispersion effects are activated, travel through the cell in a time which is equal to the free volume of the cell divided by the flow rate through the cell (a so called plug-flow). If dispersion effects are active the travel time will however be different and will also be different for different particles.

- When the particle is ready to leave the cell, it will leave through one of the cell walls that has an outgoing flow direction. The choice between cell walls with an outgoing flow is made with a likelihood that is proportional to the outflows. If several particles are traced the cloud will thus split up in proportion to the flow rates. Complete mixing in a cell is hence assumed.

It should be noted that no time is spent when moving from one cell to the neighbour. Next we will discuss some details about the two points above.

When the particles are travelling through the cell, the retardation due to matrix diffusion, sorption and Taylor dispersion need to be accounted for. The concept of particle states is used to simulate these processes. As an illustration let's outline how Taylor dispersion can be simulated. If the velocity profile is described as a number of layers, each with a certain velocity, we identify these layers as the different states a particle can be in. If correct frequencies can be ascribed for moving to a neighbouring layer, it is realised that particles will experience different velocities when travelling through the cell and a Taylor dispersion effect will result.

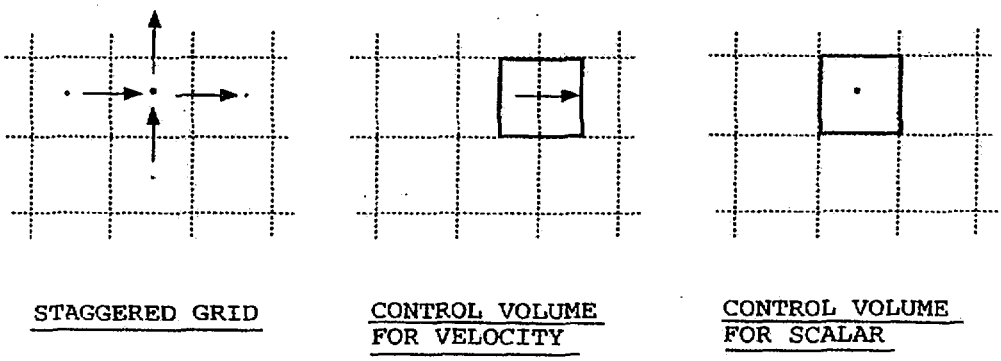


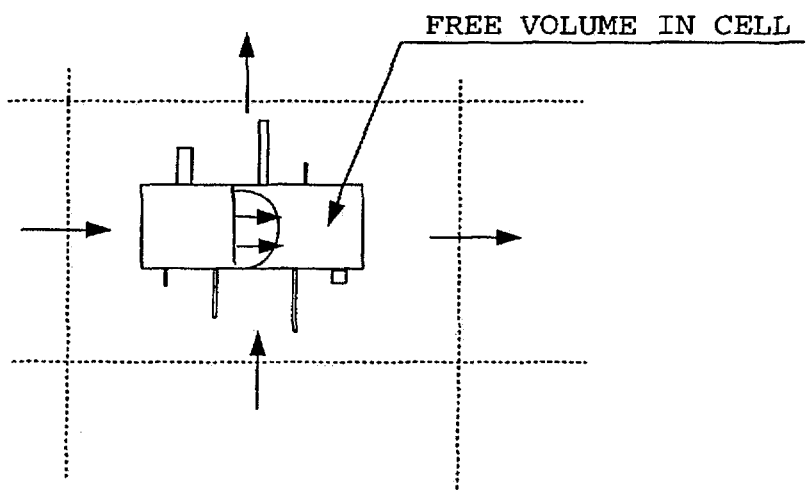


***Figure 2-2.*** *Illustration of concepts in the flow model (top) and subgrid processes affecting a particle's travel time.*

If we further should like to account for sorption on the fracture walls a particle state is also needed for this process. We also need to find out the frequency by which a particle will leave the velocity layer close to the wall and enter the "sorbed state" and also the frequency by which it will go back. Matrix diffusion is conceptualised as diffusion in a number of channels with one end in contact with the fracture. These channels can also be simulated by particle states and frequencies (details in next section).

Dispersion due to fracture intersections is simulated by the "cell-jump technique" outlined above. This method is used for each cell, but the net effect on a simulated fracture intersection is harder to estimate; a few examples are given in Figure 2-3. In the simplest possible case (thin fractures along coordinate directions) the particles will split up in proportion to the outflows. However, if the fracture intersection is at a cell-wall and the fractures make an angle to the coordinate direction it is not clear how the particle cloud will split up; it will depend on the local pressure distribution. When the fracture thickness is of the same magnitude as the grid size the situation is even more complex, as can be seen in Figure 2-3. In this case, the local flow field in the intersection is resolved and the particles will be transported accordingly. It is however not possible to say a' priori how a particle cloud will be partitioned.

It may seem discouraging that the split up of a tracer cloud in a fracture intersection is not know or controlled, even for the simple cases shown in Figure 2-3. However, as will be discussed in the test cases to be presented, it is argued that the two dimensional situations shown in Figure 2-3 are not relevant for realistic fractures. Fractures have variable aperture and it can be expected that flow channels always form. Mixing at fracture intersections is therefore related to how flow channels interact at the intersection, and hence requires a three dimensional analysis.

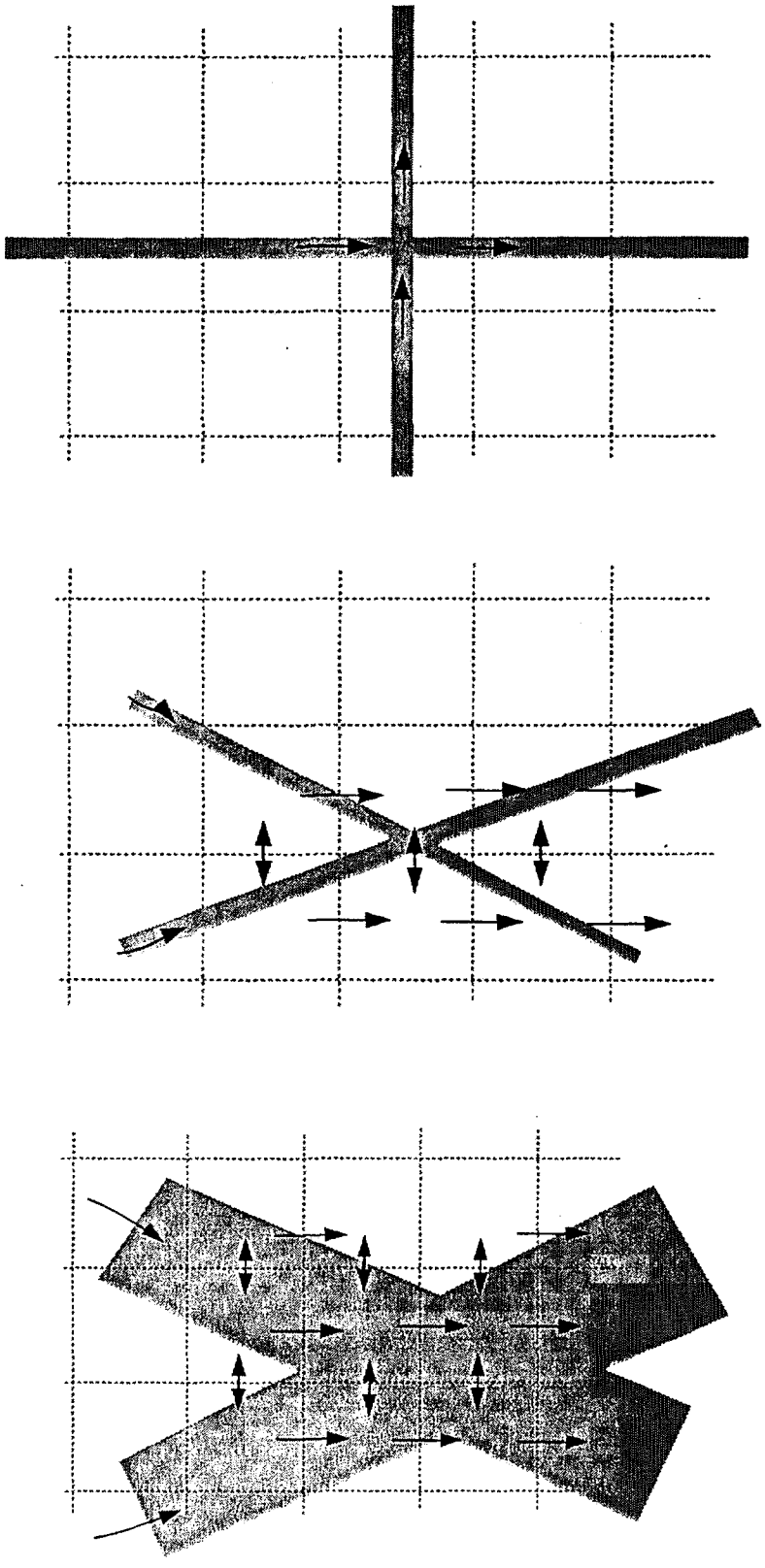

***Figure 2-3.*** *Illustration of how the flow in a fracture intersection.*

# 3 Mathematical model

## 3.1 Basic assumptions

It will be relevant to assume that the fluid is incompressible and the flow is steady for all cases to be discussed. We will further assume that the Darcy law applies and that no forces due to density gradients are present.

## 3.2 Flow model

Under the assumptions made the following equations apply:

Momentum:

$$0 = -\frac{\partial p}{\partial x} - \frac{\rho_0 g}{K_x} u \tag{3-1}$$

$$0 = -\frac{\partial p}{\partial y} - \frac{\rho_0 g}{K_y} v \tag{3-2}$$

$$0 = -\frac{\partial p}{\partial z} - \frac{\rho_0 g}{K_z} w \tag{3-3}$$

Mass balance:

$$\frac{\partial}{\partial x}\rho_0 u + \frac{\partial}{\partial y}\rho_0 v + \frac{\partial}{\partial z}\rho_0 w = 0 \tag{3-4}$$

where $u$, $v$ and $w$ are Darcy velocities, $K_x$, $K_y$ and $K_z$ conductivities, $p$ pressure, $g$ acceleration due to gravity and $\rho_0 \left(= 1000\ \mathrm{kg/m^3}\right)$ density. The coordinate directions are denoted $x$, $y$ and $z$.

## 3.3 Particle tracking

Some basic concepts about PARTRACK with multiple particle states were introduced in the previous section; now some further details will be given.

Consider the laminar velocity profile shown in Figure 3-1. In the flow model we do not simulate the velocity profile but we do get an average pore-velocity as a result of the flow calculation. The dispersion effect of the velocity profile can now be simulated by imaging a number of states a particle can be in and ascribe different velocities to each state; we may think of the states as different layers in the velocity profile, see Figure 3-1. We may also like to simulate that a particle can get sorbed on the fracture wall, which then introduces one more state a particle can be in. Let us assume that we define five states for the simulation of Taylor dispersion and one state for sorption on the fracture wall. We then need to define how a particle may move between the different states; this is done by the intensity matrix, shown in Figure 3-1. The first column gives the conditions for state one (the sorbed state). As can be seen, it only has a certain probability to move to state two, which is the first layer in the fracture. The second column gives the conditions for layer one ( state two) and so on. It can be shown, that the frequency value for change between two layers in the fracture is $D_{mol} / \Delta^2$, where $D_{mol}$ is the molecular diffusivity of the substance and $\Delta$ the layer thickness.

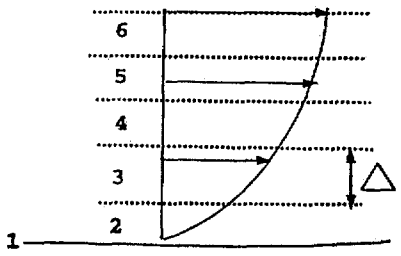


SIX PARTICLE STATES

$$\begin{pmatrix} 0 & X & 0 & 0 & 0 & 0 \\ X & 0 & X & 0 & 0 & 0 \\ 0 & X & 0 & X & 0 & 0 \\ 0 & 0 & X & 0 & X & 0 \\ 0 & 0 & 0 & X & 0 & X \\ 0 & 0 & 0 & 0 & X & 0 \end{pmatrix}$$

INTENSITY MATRIX

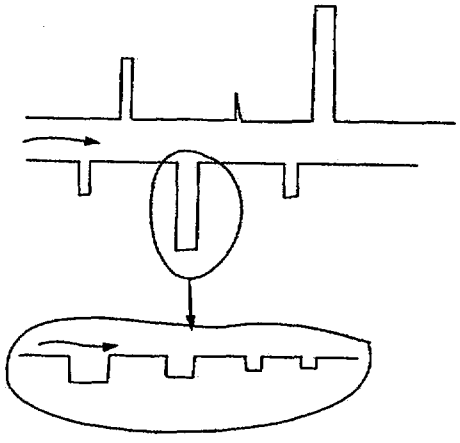

SIMULATION OF MICROFISSURES

***Figure 3-1.*** *Illustration of particle states in PARTRACK.*

If matrix diffusion in microfissures, or pores, of varying sizes and subsequent sorption on inner surfaces are to be simulated more concepts need to be introduced, see Figure 3-1. A particle that enters one of the pores, with one end in contact with the fracture, will be transported by diffusion and may get sorbed on an inner surface. To describe the one dimensional transport in the pore, we need to solve the 1D diffusion equation. It is however possible to simulate the pore by a series of boxes, see Figure 3-1. A particle that enters one of the big boxes simulates transport deep into the pore while a small box simulates a fast return to the fracture. Each box has its own "volume" or capacity and mass transfer rate coefficient. If all pores, of varying length and width, are simulated by series of boxes, continuos distributions of capacities and mass transfer rate coefficients will result. In the present model a lognormal distribution (following McKenna, 1999) of rate coefficients is used. In PARTRACK we now let each box represent one state and from the capacity and mass transfer rate coefficients we can calculate the probability that a particle will enter or leave one of the boxes. In the intensity matrix, we will only allow exchange between the boxes and the layer close to the wall in the fracture.

## 3.4 Boundary conditions

Two types of boundary condition will be used; prescribed pressure and zero mass flux. In many of the test cases a pressure difference is prescribed for two opposite faces of the computational domain and a zero flux condition is used for all other boundaries.

## 3.5 Numerical tool and output parameters

The system of flow equations is solved by the general equation solver PHOENICS (Spalding, 1981). PHOENICS is based on a finite-volume formulation of the basic equations and embodies a wide range of coordinate systems (cartesian, body-fitted, cylindrical, etc) and numerical techniques (higher order schemes, solvers etc).

The basic output parameters from the model are pressure and Darcy velocities. It is however simple to generate additional output parameters like hydraulic head.

The software for the particle tracking with multiple particle states, PARTRACK, has been developed within this project.

# 4 Results

## 4.1 Introduction

Altogether eight test cases will be presented in this section. The test cases are intended to verify and demonstrate various aspects and features of PARTRACK. The presentation of the test cases will follow a common format indicated by the subtitles: Description, Objective, Results/Discussion and Conclusion. In the Objective it will be stated if the test case is a verification or demonstration case.

The order of presentation is from simple to complex; we hence start with "transport without dispersion" continue with "hydrodynamic dispersion" followed by "multi-rate mass transport". In the final test case all processes are considered simultaneously.

## 4.2 Advection with no dispersion

Even if we idealise the fracture flow as a flow between two parallel walls, dispersion due to the velocity profile will be present (Taylor dispersion). For the test cases in this group, Taylor dispersion will however be ignored and all particles thus move with the average pore velocity.

### 4.2.1 One-dimensional advection

**Description.** The situation is outlined in Figure 4-1. All particles will be transported by advection from $x = 0$ to $x = 10.0$ metres. This is of course a trivial problem for a particle tracking routine. The reasons for including it are that, firstly, we want to ensure that the simplest possible test case works and, secondly, it introduces the typical geometry and parameters that will be used for all test cases. We will hence use the simple geometry shown for more complex test cases. For this case we do not need to use the flow model; the velocity is simply given as an input parameter. A value of $10^{-4}$ m/s was used.

**Objective.** Verify that the simplest possible test case works and introduce the typical geometry and parameters to be used in more complex cases.

**Results/Discussion.** The calculated breakthrough curve is shown in Figure 4-1. All particles arrive after 27.8 hours, which is in agreement with the expected time. As mentioned, PARTRACK

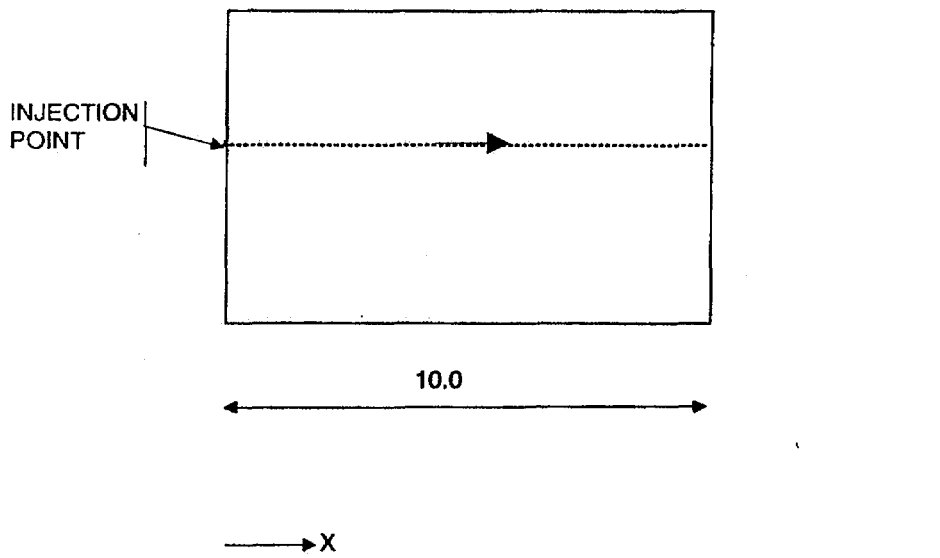


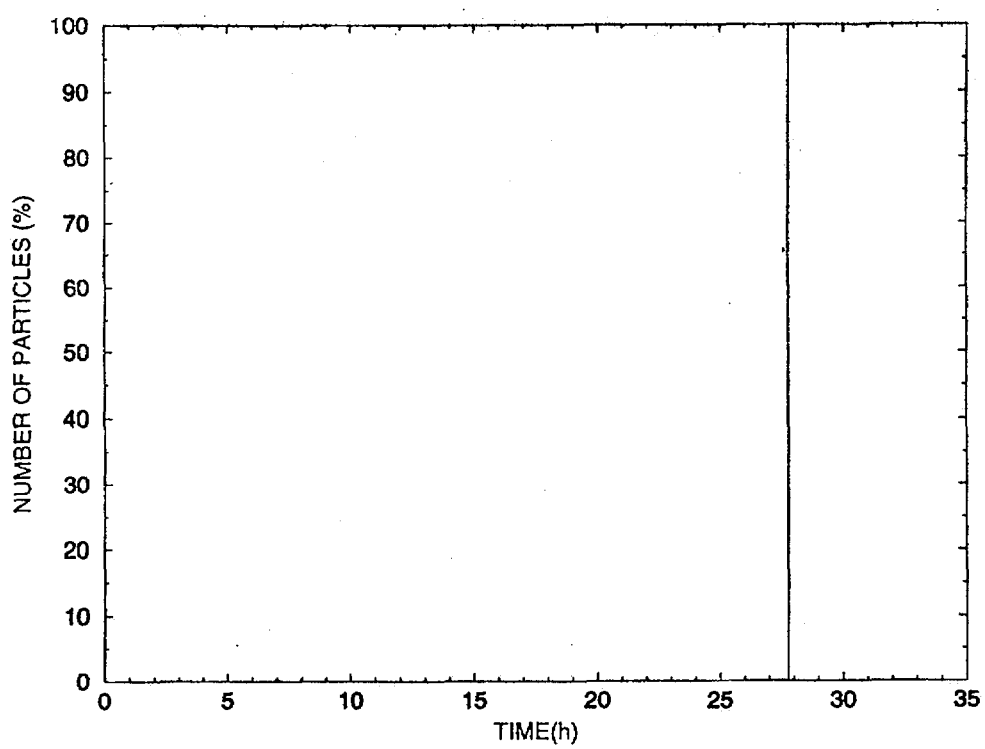


***Figure 4-1.*** *One-dimensional advection. Situation considered (top) and breakthrough curve.*

uses a grid system; in the present case a cell size, $\Delta$, of 0.025 metre was used.

**Conclusion.** The arrival time for particles in a single fracture, transported by the mean velocity, is in agreement with the analytical solution.

### 4.2.2 A fracture network

**Description.** The two dimensional fracture network considered next is shown in Figure 4-2. A pressure gradient is applied, to give a flow from left to right with a pore velocity of about $10^{-4}$ m/s.

This case is of interest for the following reasons:

- It is possible to determine the flow in each part of the fracture network analytically.
- The transport time for a particle is known, whatever path it takes.
- If we assume complete mixing in fracture intersections, one can determine analytically how a cloud of particles, injected at the upstream side, will leave through the outlets.
- As we solve for the flow and calculate the kinematic porosity field (assuming a certain fracture kinematic porosity) we get an opportunity to test the integration between PARTRACK and the flow solver.

The analytical solution gives the flow-rates in each of the fracture sections. If we inject a cloud of particles in fracture B-B, it will split up in fracture intersections in proportion to the flow rates (assuming complete mixing in fracture intersections). These fractions are given in Figure 4-2, assuming that all fractures have the same transmissivity. From the analytical solution we can thus get both the arrival time and size of each breakthrough pulse. In the numerical solution of the flow field we assume that the kinematic porosity of the fractures is equal to 0.05. The fracture thickness, $b$, will be varied in order to test a range of ratios $b/\Delta$, where $\Delta$ is the grid size (equal to 0.1 metre). In all simulations $10^5$ particles were injected in fracture B-B.

**Objective.** The main objective is to verify that the numerical solution is in agreement with the analytical one. It is a part of this objective to test the integration between the flow solver and PARTRACK and to evaluate the sensitivity to the ratio $b/\Delta$.

**Results/Discussion.** We first calculate the flow and porosity fields by the flow model. A cloud of particles, injected in fracture B-B, is then tracked by PARTRACK. The result can be studied in Figure 4-3. In order to understand the result one may first note that the transport time in fracture B-B is 27.8 hours and that all other pathways have longer transport times. The size of the pulses is explained by noting that 100% enters in fracture B-B, about 50% go each way in each crossing. The first pulse that leaves fracture B-B will thus contain about 25% of the injected pulse. It will however not be exactly 25% as the flow rates in the fracture sections are not exactly the same. As seen in Figure 4-3, the numerical solution is in good agreement with the analytical solution. One may question why we do not get an exact agreement. The answer is probably that we do not get the assumed split up of the particle cloud in fracture intersections. In the analytical solution we assumed that the cloud will split up in proportion to the outflows. In the numerical solution, see Figure 2-3, we solve for the flow and transport in the intersection. The effect can be noted in the intersection between fractures A-A and C-C. The particles arrive in fracture A-A and should split up in about equal fractions in the two outlets. From Figure 4-3 it is seen that the numerical solution gives fewer particles in fracture A-A, as compared to the analytical solution. This is probably due to the local flow pattern in the fracture intersection. In the literature, see for example Park and Lee (1999), two concepts for solute transport in a fracture intersection are used; "complete mixing" and "streamline routing". The effect described is due to streamline routing in the fracture intersection. It should however be noted that these concepts are adequate only for fractures of constant aperture. Fractures with varying aperture, to be discussed below, may require a different description.

The results given in Figure 4-3 are based on a fracture thickness, $b$, of 0.05 m $(b/\Delta = 0.5)$. The sensitivity to the fracture width is presented in Table 4-1, where results for $b/\Delta = 0.1,\ 0.5,\ 1.0$ and 2.0 are given. It is seen that the transport time does not vary strongly with $b/\Delta$, while the size of the breakthrough pulse depends strongly on $b/\Delta$ (see for example fracture A-A). As discussed above, this is due to the two dimensional representation of the fracture intersection, see also Figure 2-3.

**Conclusion.** The transport times for a simple two dimensional fracture network are in agreement with the analytical solution. The simulated partitioning of a particle cloud in a fracture intersection is close to complete mixing for small fracture thicknesses, while the streamline routing effect is important when $b > \Delta$.

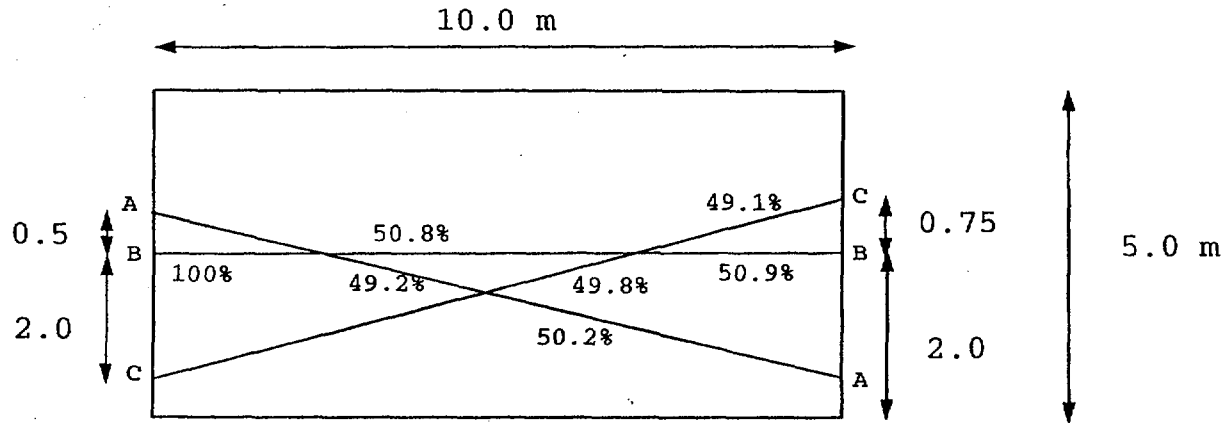


***Figure 4-2.*** *A fracture network. Outline of situation studied. The %-figures give the proportions for the split-up of a tracer cloud at the three fracture intersections (assuming complete mixing).*

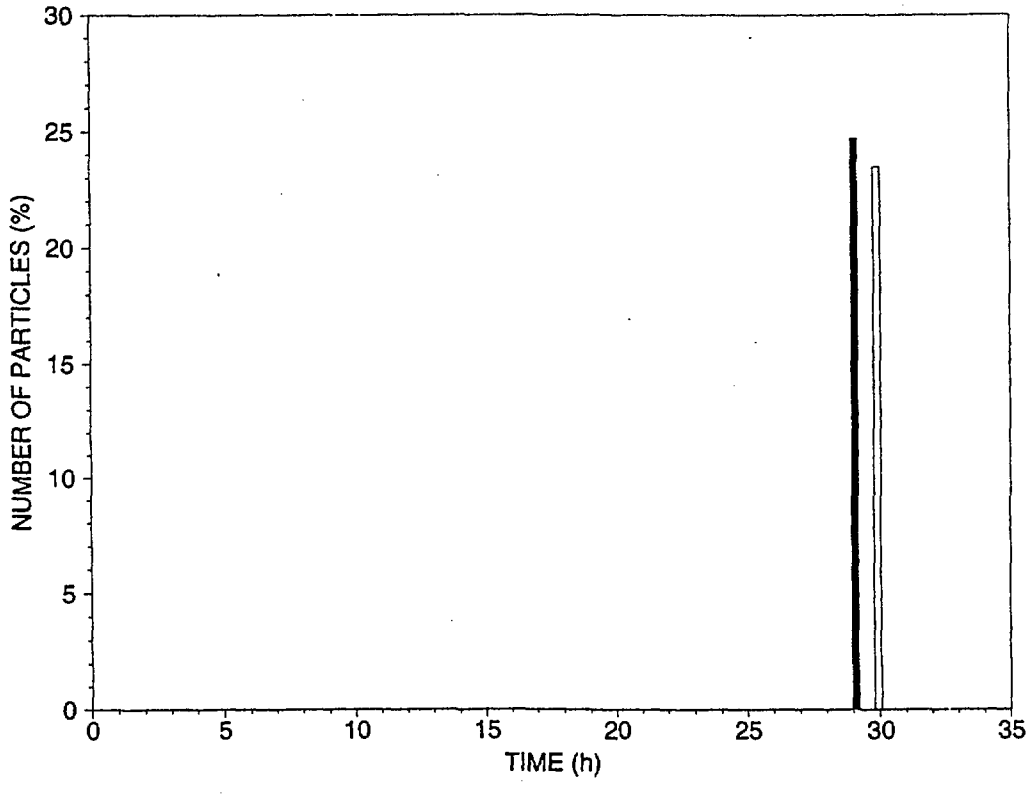


***Figure 4-3.*** *A fracture network. Breakthrough curve in fracture A-A. Solid bar gives the analytical solution.*

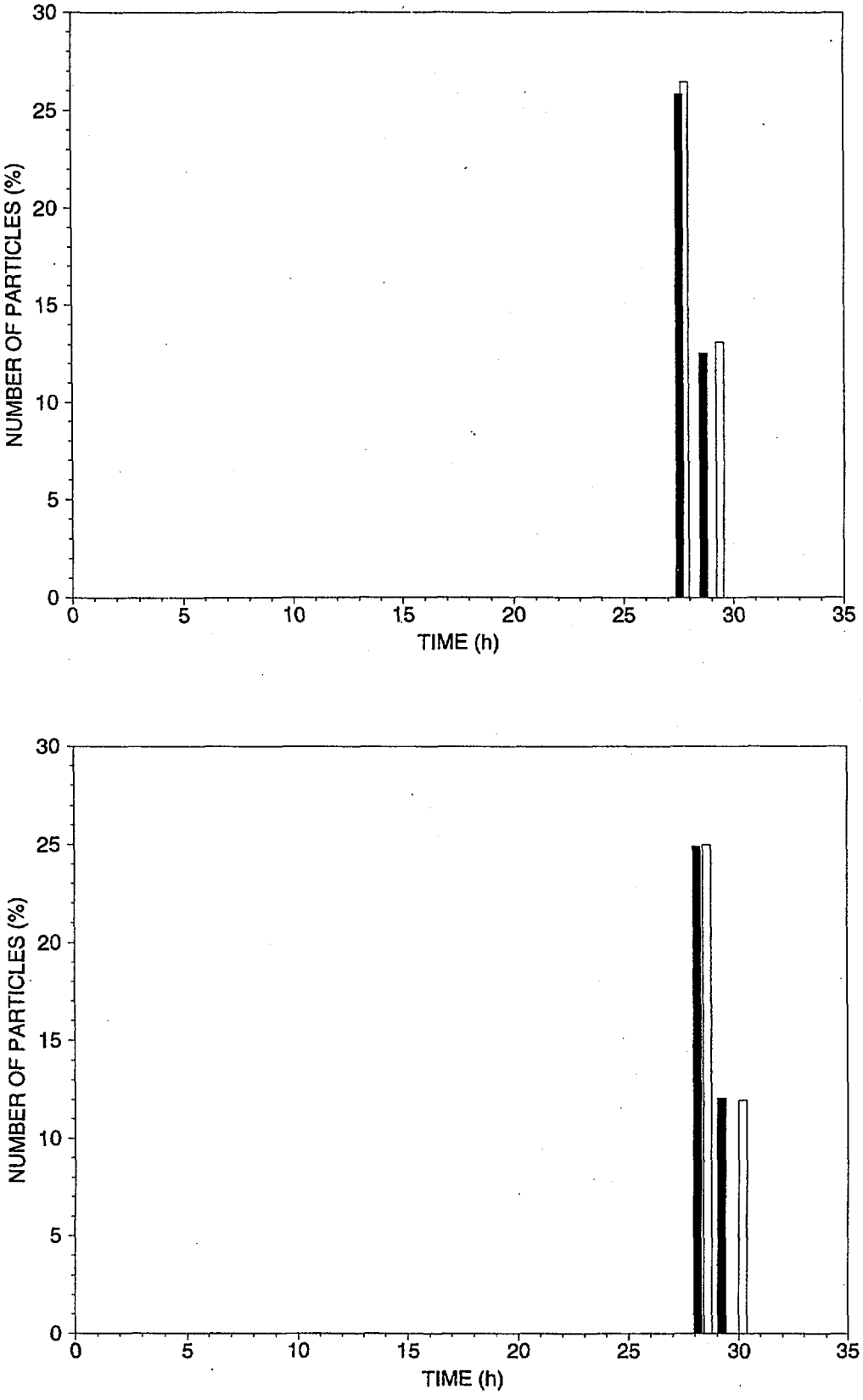


***Figure 4-3. Cont.*** *Breakthrough curves in fractures B-B (top) and C-C.*

**Table 4-1. A fracture network. Breakthrough curves (time, *t*, and fraction, *f*) in various fracture outlets as a function of normalised fracture thickness ($b/\Delta$).**

| Breakthrough curve in fracture | Analytical solution | | Fracture thickness normalised with $\Delta$ ($b/\Delta$). | | | | | | | |
|---|---|---|---|---|---|---|---|---|---|---|
| | | | 0.1 | | 0.5 | | 1.0 | | 2.0 | |
| | $t_a$(h) | $f_a$(%) | $t/t_a$ | $f/f_a$ | $t/t_a$ | $f/f_a$ | $t/t_a$ | $f/f_a$ | $t/t_a$ | $f/f_a$ |
| A-A | 29.2 | 24.7 | 1.02 | 0.94 | 1.02 | 0.95 | 1.00 | 0.75 | 1.00 | 0.50 |
| B-B | 27.7 | 25.8 | 1.00 | 1.02 | 1.00 | 1.02 | 1.00 | 1.01 | 0.99 | 0.90 |
| B-B | 28.8 | 12.5 | 1.01 | 1.06 | 1.01 | 1.05 | 0.98 | 1.20 | 0.95 | 1.87 |
| C-C | 28.3 | 24.9 | 1.01 | 1.00 | 1.00 | 1.00 | 1.00 | 1.09 | 1.00 | 1.00 |
| C-C | 29.4 | 12.1 | 1.02 | 0.99 | 1.02 | 0.99 | 1.01 | 1.09 | 1.00 | 1.31 |

### 4.2.3 A single fracture in a 3D domain

**Description.** This test case is the same as used in Svensson (1999a), to evaluate how the flow rate through a single fracture varied with the orientation and thickness of the fracture. The situation studied is outlined in Figure 4-4. The pressure is held constant on two opposite faces ($y = 0.0$ m and $y = 10.0$ m) and a zero flux condition is used on all other boundaries. At the inflow boundary the position of the fracture is fixed, with centreline coordinates (1.0, 0.0, 1.0). The fracture position at the downstream boundary is varied in order to test a wide range of angles to the coordinate directions. Also a range of thicknesses were tested, but the height of the fracture was kept constant at 0.5 metres.

For each of the situations studied, a steady state flow calculation is first performed. PARTRACK is then used to calculate the transport time from the inlet to the outlet.

**Objective.** Verify that PARTRACK gives correct transport times for fractures of different thicknesses and orientations. As the flow and porosity is calculated in the flow model, the test case also evaluates the integrated performance of the flow and transport model.

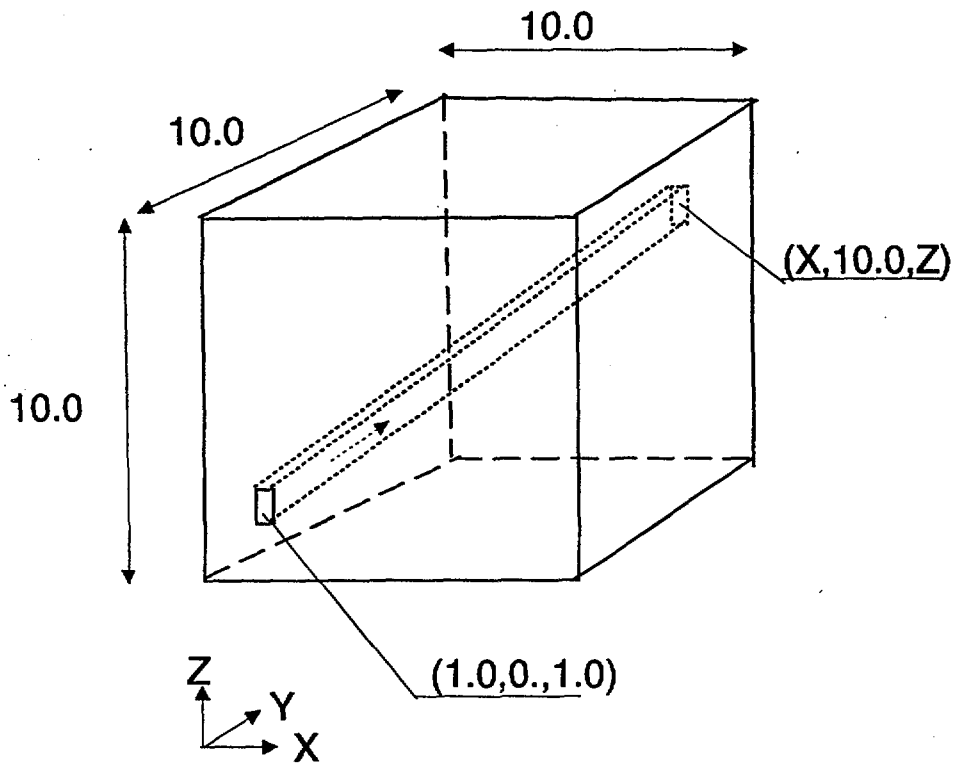


*Figure 4-4. A single fracture in a 3D domain. Outline of situation studied. All distances in metres.*

**Results/Discussion.** Results are presented in Table 4-2. Five downstream fracture positions and four fracture thicknesses were tested. The five downstream fracture positions will give a fracture that, for the first position, is parallel to the $y$- coordinate while the last position gives a fracture that almost follows a diagonal in the box. Note also that the $x$ and $z$ coordinates for the downstream positions are different; this ensures that the fracture will have different angles to all three coordinate directions (except for the first position). The transport times are normalised with the analytically determined transport time, $t_a$, which is easily obtained from the specified pressure gradient, kinematic porosity and fracture length.

**Table 4-2. A single fracture in a 3D domain. Transport time as represented in the grid, $t$, normalised with the true transport time, $t_a$, for various fracture thicknesses and orientations.**

| Fracture coordinates at downstream boundary [m] | Analytically determined transport time, $t_a$ [h] | Transport time ($t/t_a$) Fracture thickness ($b/\Delta$) | | | |
|---|---|---|---|---|---|
| | | 0.1 | 0.5 | 1.0 | 2.0 |
| X = 1.0, Z = 1.0 | 27.50 | 1.00 | 1.00 | 1.00 | 1.00 |
| X = 3.0, Z = 2.5 | 29.02 | 1.06 | 1.02 | 1.01 | 1.00 |
| X = 5.0, Z = 4.0 | 34.37 | 1.08 | 1.03 | 1.01 | 1.00 |
| X = 7.0, Z = 5.5 | 42.97 | 1.04 | 1.02 | 1.01 | 1.00 |
| X = 9.0, Z = 7.0 | 54.98 | 1.02 | 1.01 | 1.00 | 1.00 |
| | Average | 1.04 | 1.02 | 1.01 | 1.00 |

From Table 4-2, one may conclude that accurate transport times are calculated provided $b/\Delta$ is not too small; if $b/\Delta$ is larger than 0.5 the error is less than 3%. In Svensson (1999a) it was found that the flow rate through a single fracture in a 3D domain was underpredicted with a few percent. The error in the transport times is thus mainly due to the error in the flow rates, which can be concluded from a comparison with Table 4-2 in Svensson (1999a).

It is also of interest to note that the spread of the breakthrough curve in all simulations was small. Ideally all particles should arrive at the same time, but some numerical dispersion is present as particles will have different flow paths. The standard deviation of the breakthrough curve was however always less than 2% of the transport time and the numerical dispersion effect is hence small (as compared to other effects to be discussed).

**Conclusion.** Accurate transport times are calculated for a single fracture of varying thickness and orientation in a 3D domain, provided the fracture thickness in relation to the grid size is not too small. If $b/\Delta > 0.5$, the maximum error in the calculated transport time is found to be less than 3%.

## 4.3 Hydrodynamic dispersion

In Section 2, a number of processes causing a broadening of the breakthrough curve are discussed. One reason for this broadening is that particles may take different flow paths and hence get different transport times. We call this spreading of the particle cloud hydrodynamic dispersion. A closer examination, see Section 2, shows that hydrodynamic dispersion is due to, at least, the following processes: at fracture intersections a split up of a particle cloud may occur, in a fracture plane channelling gives different transport times and the velocity profile between two fracture walls cause a longitudinal spread of a particle cloud. These processes will now be studied one by one.

### 4.3.1 Taylor dispersion

**Description.** The basic idea of Taylor dispersion has already been introduced, see Figures 2-1 and 3-1. If a cloud of particles is introduced in a fully developed flow between two parallel walls, the particles will be dispersed longitudinally at a rate given by (Sahimi, 1995):

$$D_L = \frac{2}{105}\frac{h^2 u^2}{D_m} \tag{4-1}$$

where $D_L$ is the longitudinal dispersion coefficient, $h$ half the aperture, $u$ the mean velocity and $D_m$ the molecular diffusion coefficient of the solute the particles represent. When we use PARTRACK to simulate Taylor dispersion we subdivide the space between the two walls into five layers and each layer is considered as a state a particle can be in, see Figure 3-1. The simple geometry given in Figure 4-1 is used for this test case.

**Objective.** Verify that PARTRACK predicts Taylor dispersion correctly. As this test case uses the multiple particle state feature of PARTRACK, it is an important test as it evaluates if this feature is correctly implemented.

**Results/Discussion.** Three runs, with $D_m$ equal to $10^{-9}$, $10^{-10}$ and $10^{-11}$ $m^2/s$ respectively, were carried out in order to compare the simulated dispersion with Equation 4-1. The result can be studied in Figure 4-5. From the breakthrough curves the mean arrival time and the standard deviation, $\sigma$, was calculated. The standard deviation is then related to the longitudinal dispersion coefficient, $D_L$ ( $s = \sqrt{2D_L t}$, where $t$ is the mean transport time). As can be seen a perfect agreement between the analytically determined and

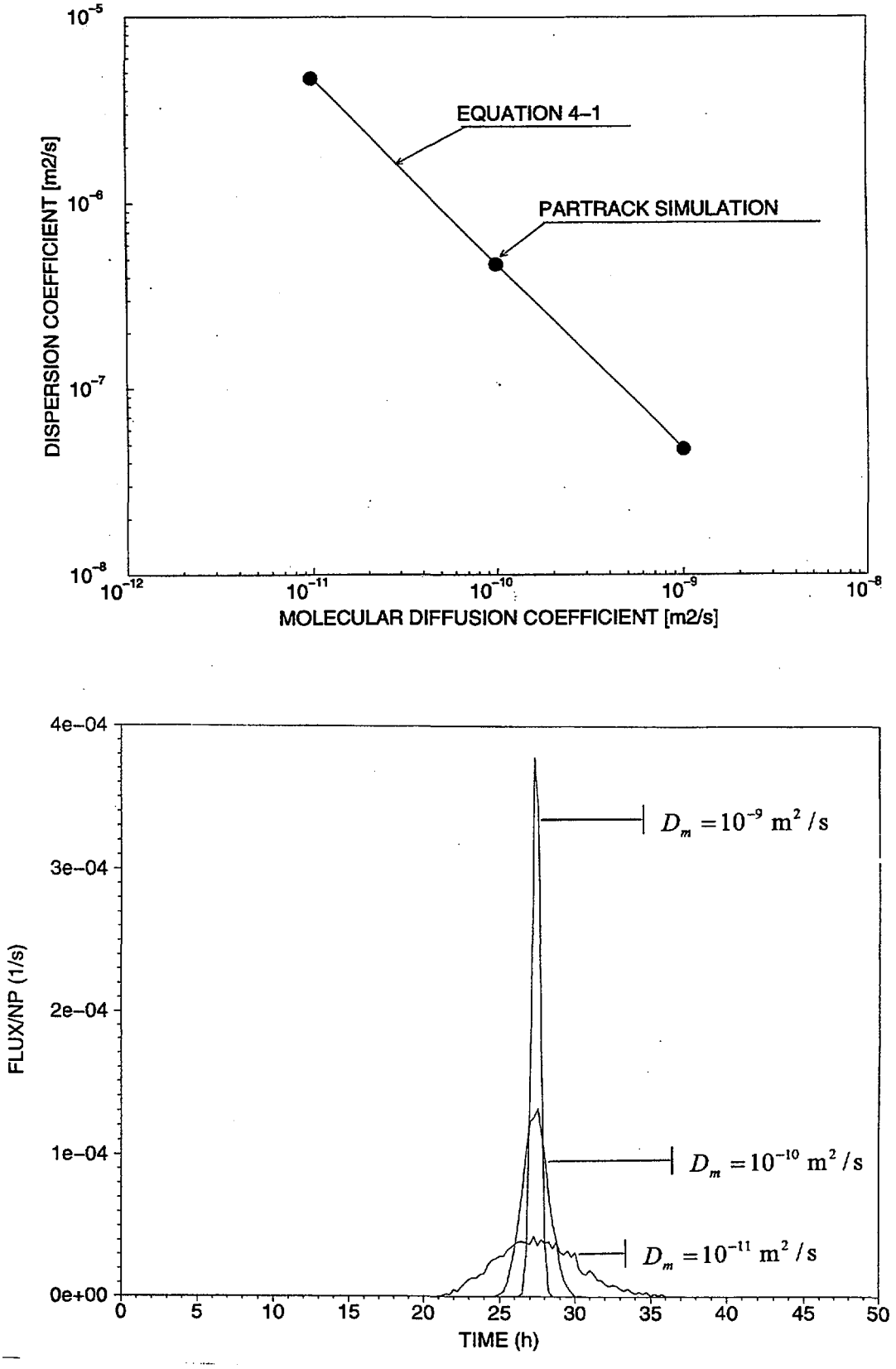


***Figure 4-5.*** *Taylor dispersion in a single fracture. Comparison with Equation 4-1 (top) and breakthrough curves.*

simulated dispersion is obtained. This result is important as it shows both that PARTRACK with multiple particle states works and that Taylor dispersion can be simulated correctly. The breakthrough curves, also shown in Figure 4-5, show that the Taylor dispersion effect is small for $D_m = 10^{-9}$ m$^2$/s, while a significant spread is obtained for $D_m = 10^{-11}$ m$^2$/s. This result is of course related to the parameters and geometry used in this test case.

**Conclusion.** The results presented show that PARTRACK, with multiple particle states, works correctly and that the predicted Taylor dispersion is in perfect agreement with the analytical solution.

### 4.3.2 Channelling

**Description.** Next we will investigate the dispersion properties of a fracture with variable aperture, and hence also transmissivity. The situation studied is outlined in Figure 4-6. The algorithm used for generating a fracture plane with a certain correlation structure in the aperture field is described in Kuylenstierna and Svensson (1994). In that report the mathematical background, the computer code as well as applications can be found. Applications were however strictly two dimensional, i.e. only one plane was studied at the time. As part of the present project a method to "plant" the fracture plane into a three dimensional grid has been developed. This will allow for several fractures, with individual properties, to interact (i.e. fracture intersections). In the present test case only a single fracture will be studied, but the grid is three dimensional. The only reason for using a three dimensional grid is however that we want to test the method developed. A uniform grid with grid size 0.05 metre was used in this case.

A series of simulations, where the properties of the aperture field are varied, will be presented. First a flow simulation is performed, then PARTRACK is used to simulate the transport of a cloud of particles injected at the middle of the inlet section, see Figure 4-6.

**Objective.** There are two main purposes of this test case. First, we want to demonstrate that a fracture with varying properties can be planted into a three dimensional grid. Second, it is the intention to show how the dispersion properties, i.e. the effect on the breakthrough curve, may vary with the fracture properties. It should be noted that this is the first test case presented as a demonstration case. We will hence not attempt any verification, but instead emphasise that the flow and transport codes have the capacity to simulate the processes addressed.

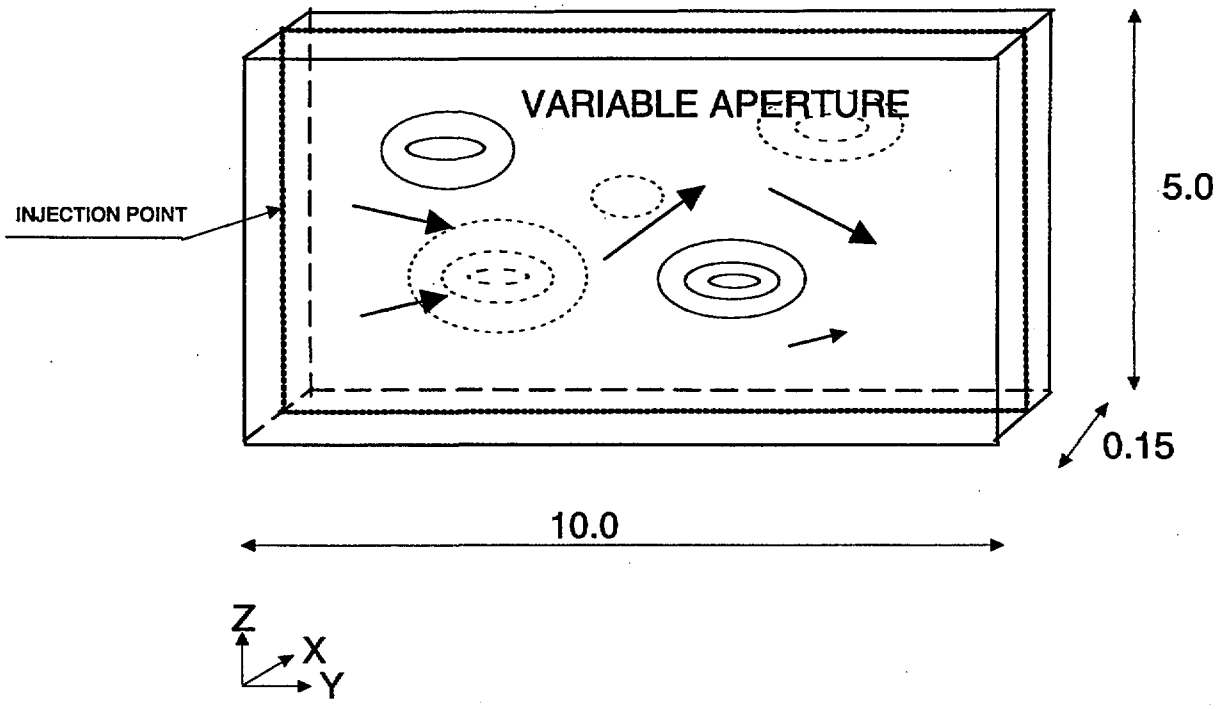


***Figure 4-6.*** *Channelling in a fracture due to an aperture field with a certain correlation structure. The ellipses in the figure indicate a variable aperture.*

**Results/Discussion.** Altogether four simulations will be presented. First a reference case is defined and then variations of this case are studied. The four cases can be described as follows:

- Reference case. The mean transmissivity, $T$, is equal to $10^{-6}$ $m^2/s$ and its $\log_{10}$ standard deviation 1.5. The mean aperture, $e_T$, is calculate from $e_T = 1.428 \times T^{0.523}$ (Rhén et al., 1997), giving a mean aperture of $10^{-3}$ m . The $\log_{10}$ standard deviation of $e_T$ will be 0.78, due to the variation in $T$. The correlation length is set to 0.30 m and the distribution is isotropic.

- Case A. The $\log_{10}$ standard deviations for $T$ and $e_T$ are increased by a factor of 2.0.

- Case B. The correlation length is reduced with a factor of 2.0.

- Case C. The correlation structure is anisotropic, with the two correlation lengths 0.15 and 0.45 metres and with a tilt of 45° degrees to the main flow direction.

The conductivity distributions for these four cases are given in Figure 4-7. The distributions represent the cell layer that the fracture cuts through. Note that the reference case and Case A will have a similar appearance, but a different span in the conductivity values. The steady state flow field is then calculated for the four cases and PARTRACK is used to simulate the transport of a cloud of particles injected at the inlet boundary. The breakthrough curves at the outlet side can be studied in Figure 4-8. A striking feature of this figure is that the breakthrough curve for Case A is significantly delayed and more dispersed than the other curves. The explanation for this is probably that the injection point is located in an area with a smaller than average aperture. When the standard deviation is increased the injection point gets more isolated. The delay is hence due to the transport from the injection point to the first flow channel. Another realisation of the conductivity field could have placed a flow channel at the injection point. For such a situation, it is expected that case A should get a much shorter mean arrival time. It is thus not possible to draw any general conclusions about dispersion in a fracture with varying aperture, from a single realisation of the conductivity field.

**Conclusion.** It has been demonstrated that a fracture with varying properties in the fracture plane can be represented in a three dimensional grid. It has further been shown how the breakthrough curve can be modified due to these varying properties.

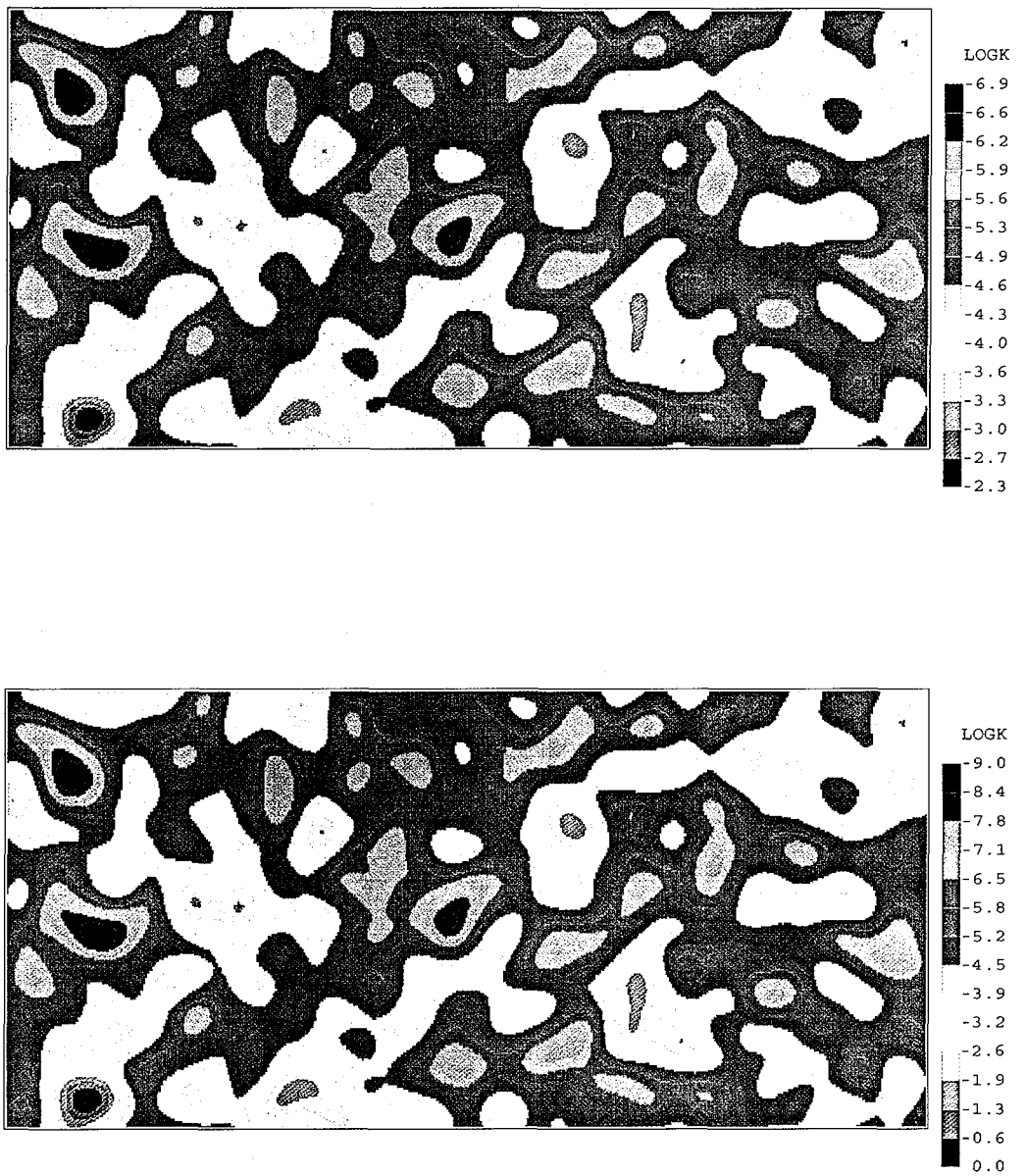


***Figure 4-7.*** *Channelling. Conductivity distributions for the reference case (top) and Case A.*

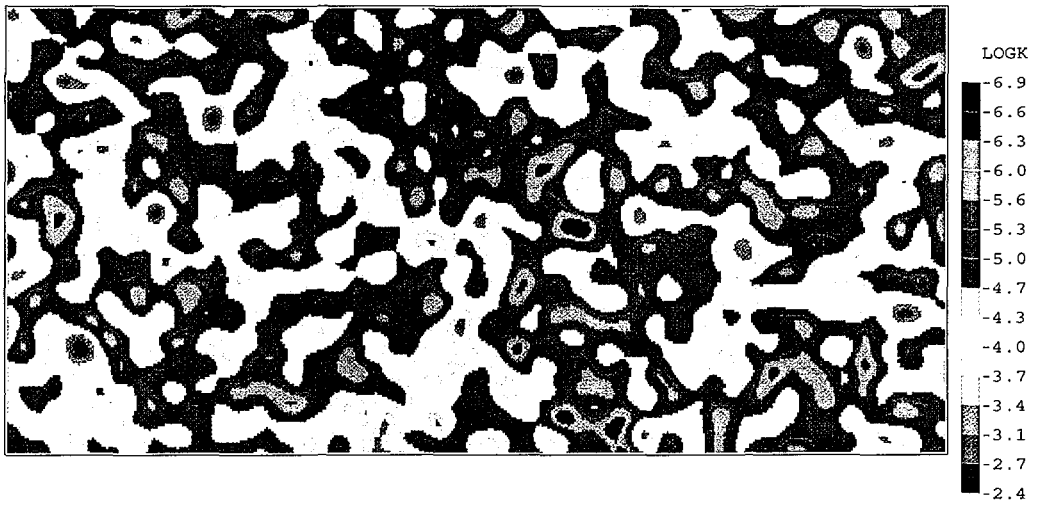


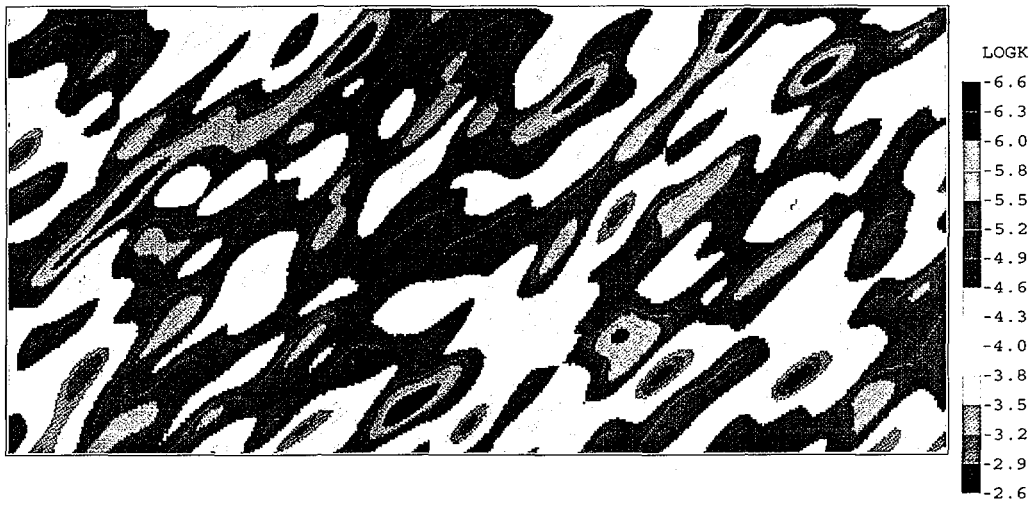


***Figure 4-7. Cont.*** *Case B (top) and Case C.*

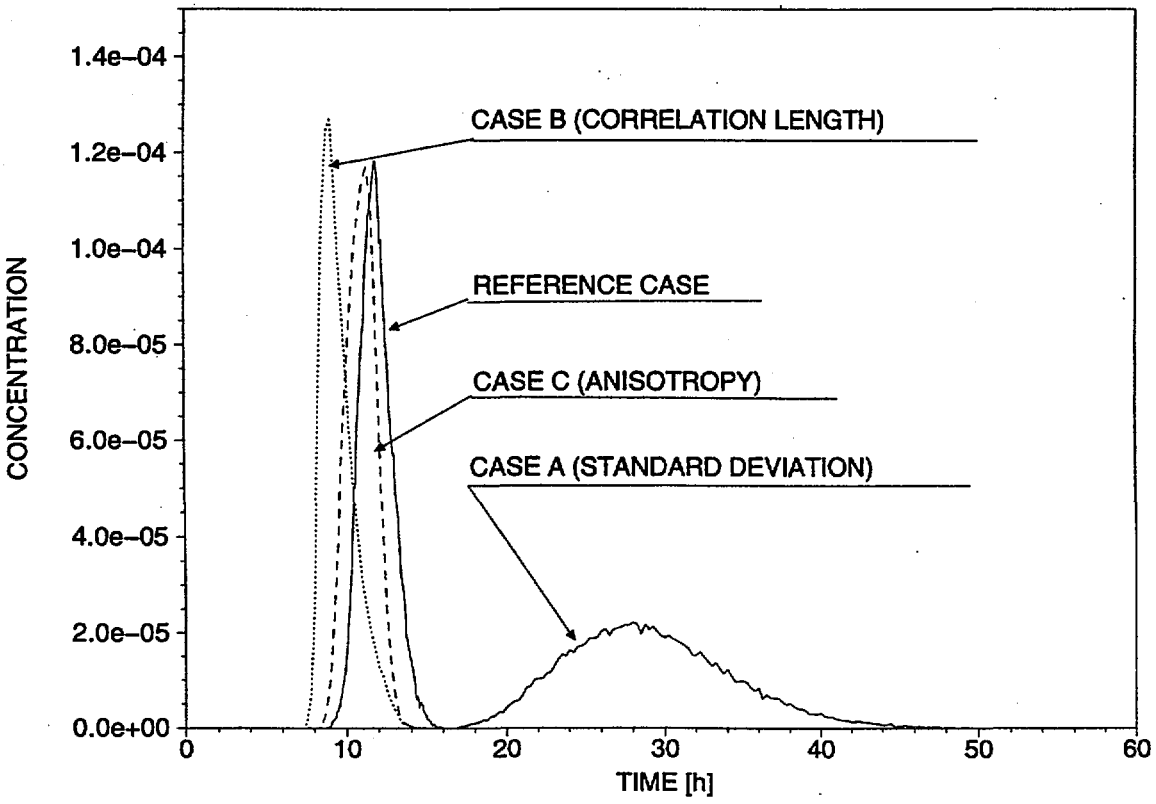


***Figure 4-8.*** *Channelling. Breakthrough curves for the four cases studied.*

### 4.3.3 A fracture intersection

**Description.** Above it was mentioned that two concepts are used to describe transport in a fracture intersection "complete mixing" and "streamline routing" (Park and Lee, 1999). It was also questioned if these concepts are adequate, as they seem to regard the problem as being two dimensional.

In the previous test case, it was demonstrated that a fracture with an aperture distribution can be represented in a three dimensional grid. By specifying two crossing fractures with variable aperture, it should be possible to get a more accurate description of the mixing properties of the fracture intersection. It is easy to imagine that a channel in one fracture may continue in the crossing fracture. One channel may also continue through the crossing fracture unaffected, if it crosses an area of low transmissivity. It may hence be the case that mixing in a fracture intersection is more related to how flow channels interact, than to the two concepts mentioned above.

In Figure 4-9, a situation with two crossing fractures is outlined. A pressure gradient will be applied in the $x$ and $y$ directions giving an equal flow in the two fractures. First the flow field is calculated then a cloud of particles is injected in one of the fractures. For a number of realisations of the aperture field, we study the number of particles that depart into the crossing channel.

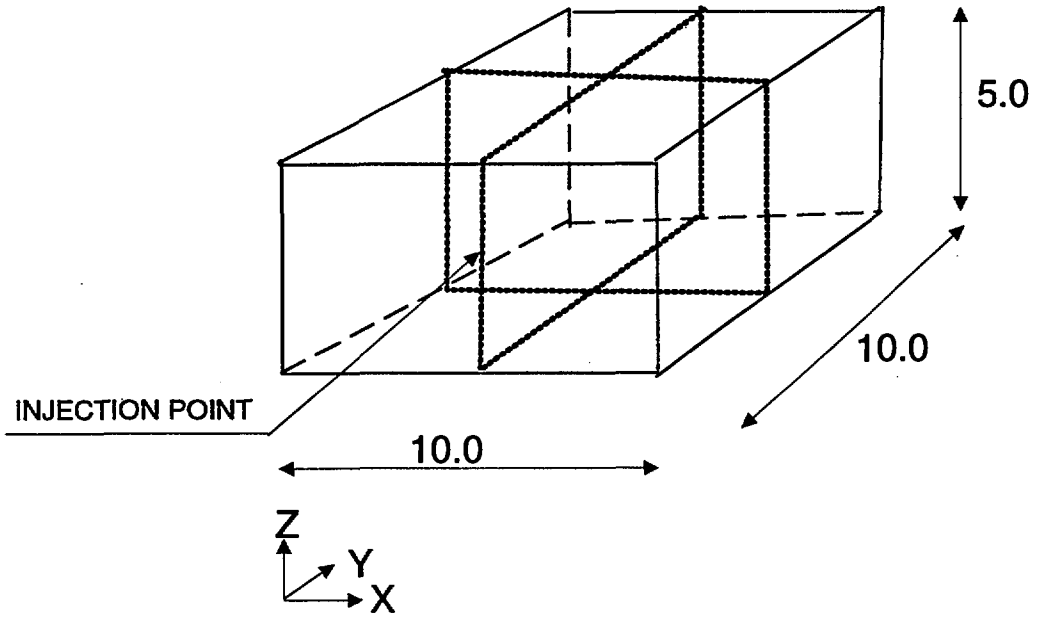


***Figure 4-9.*** *A fracture intersection. Outline of situation studied.*

**Objective.** Demonstrate and discuss a method to analyse the transport properties of a fracture intersection.

**Results/Discussion.** The two fractures are generated as two realisations, using the following specification:
Mean transmissivity = $10^{-6}$ m$^2$/s, standard deviation of $\log_{10} T = 1.0$, mean aperture = $10^{-3}$ m, standard deviation of $\log_{10} e_T = 0.5$ and isotropic correlation structure with correlation length 0.3 metre. When the two fractures are represented in the grid, conductivities are added in the cells where both fractures are present. This can be seen in the two cutting planes shown in Figure 4-10. At the fracture intersection a line of somewhat higher conductivities are found and there is also a tendency for a flow along the intersection. A closer examination of the flow field also shows that some flow channels start in one fracture and continues in the crossing one.

In order to study the transport properties of the intersection, particles were injected at the inlet of one of the fractures and tracked through the domain. It was noted if a particle left the domain through the same fracture as it was injected in, or if it left through the crossing one. Using $10^5$ particles and 20 realisations of the fracture geometries it was found that 48% of the particles departed to the crossing fracture at the intersection. Large variations between different realisations were however found and the result should therefore be interpreted as "about 50% departed to the crossing fracture".

The results presented are only intended to point to a way to analyse how a fracture intersection may cause a dispersion effect. It is suggested that the interaction between flow channels in the two fractures is the key to understanding the mechanism. The flow and transport codes used here have the capability to simulate many interesting variations of the present test case (anisotropy, different fracture orientations, etc).

**Conclusion.** It is questioned if the traditional concepts of transport in a fracture intersection are adequate. As an alternative, it is suggested that it is the interaction between flow channels in the two fractures that should be in focus. A method to analyse the transport properties of a fracture intersection from this point of view has been demonstrated.

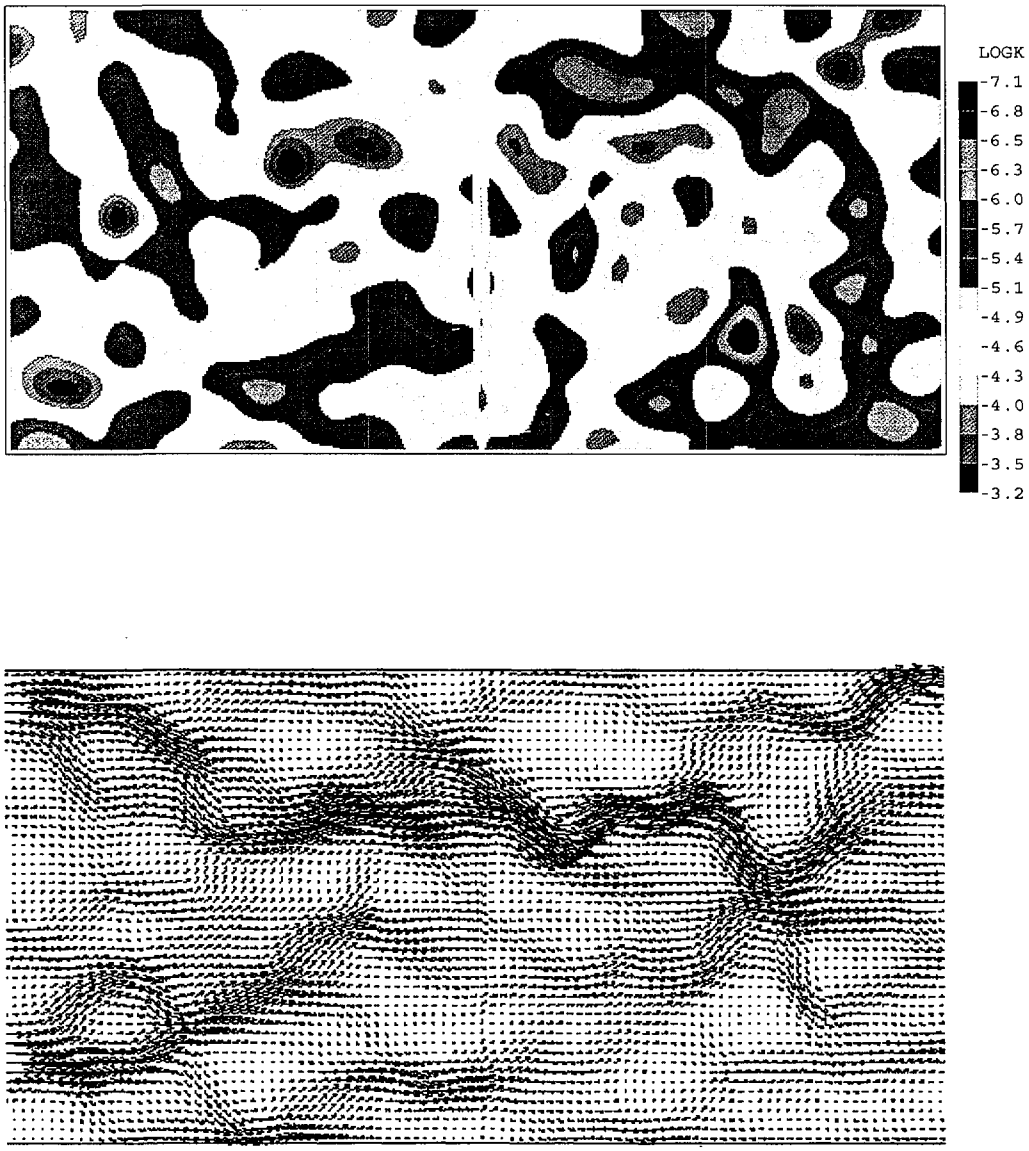


***Figure 4-10.*** *A fracture intersection. Conductivity and flow distribution in a plane aligned with one of the two fractures.*

## 4.4 Matrix diffusion and sorption

Mass transport processes will be simulated with the multi-rate mass transfer method described earlier. Within the TRUE-project, McKenna (1999) has applied a multi-rate model to a tracer experiment at Äspö. We will use the parameters estimated by McKenna (1999), but the objective is not to apply PARTRACK to field data. Instead an intercomparison between PARTRACK and the multi-rate model as formulated by McKenna (1999) will be in focus.

### 4.4.1 Multi-rate model for a one dimensional pathway

**Description.** Once again, we will use the simple flow geometry given in Figure 4-1, i.e. a single fracture of constant aperture. There is no need to calculate the flow field for this case; the transport velocity is simply specified to $10^{-4}$ m/s. In the model used by McKenna, a constant dispersivity $(\alpha_L = 0.2\ \mathrm{m})$ was used to simulate longitudinal dispersion. In the present simulations we assume that Taylor dispersion is the cause of longitudinal dispersion. In order to get the same longitudinal spread $\alpha_L \times U$ should equal $D_L$, as given by Equation 4-1; $D_m = 2.4\times10^{-11}$ m$^2$/s will give this effect.

Breakthrough curves for a number of tracers were calculated by McKenna (1999) and parameters needed in the multi-rate model were estimated. In the present comparison we will choose three tracers (HTO, Sr85, Rb86) and use the parameters estimated by McKenna for these. The injection is specified as a Dirac pulse, i.e. all the tracer is injected instantaneously.

**Objective.** Verify that PARTRACK predicts the same breakthrough curves as the multi-rate model by McKenna (1999), for a range of tracers with strongly varying sorptivity.

**Results/Discussion.** The tracer input parameters are given in Table 4-3. In this table $\beta_{tot}$ denotes the total capacity coefficient, $R_m$ the retardation factor and $\mu$ and $\sigma$ the mean and standard deviation of the lognormal probability density function, defining the distribution of mass-transfer rate coefficients; see McKenna (1999) for further details.

**Table 4-3. Input parameters for the multi-rate model (from McKenna, 1999).**

| Tracer | $\beta_{tot}$ | $\mu$ | $\sigma$ | $R_m$ |
|---|---|---|---|---|
| HTO | 6.65 | -16.4 | 0.385 | 1.00 |
| Sr85 | 42.7 | -20.7 | 4.40 | 0.92 |
| Rb85 | 98.1 | -17.7 | 2.15 | 2.10 |

In PARTRACK these distributions are discretized into a number of boxes, each with its own capacity and mass transfer coefficient. Depending on the distributions of capacities and mass transfer coefficients, the number of boxes can vary from tens to hundreds.

Comparisons of the breakthrough curves can be found in Figure 4-11. It should be mentioned that the breakthrough curves calculated by PARTRACK were scaled to have the same integrated mass flux as the curves given by McKenna's model. It is anyway clear that PARTRACK, with the multiple particle state feature, is in close agreement with the model by McKenna. The difference is limited to early arrival times, which may be caused by the different concepts used to handle longitudinal dispersion. In PARTRACK it is attributed to Taylor dispersion, while the method by McKenna uses a more traditional diffusion-like parameterisation.

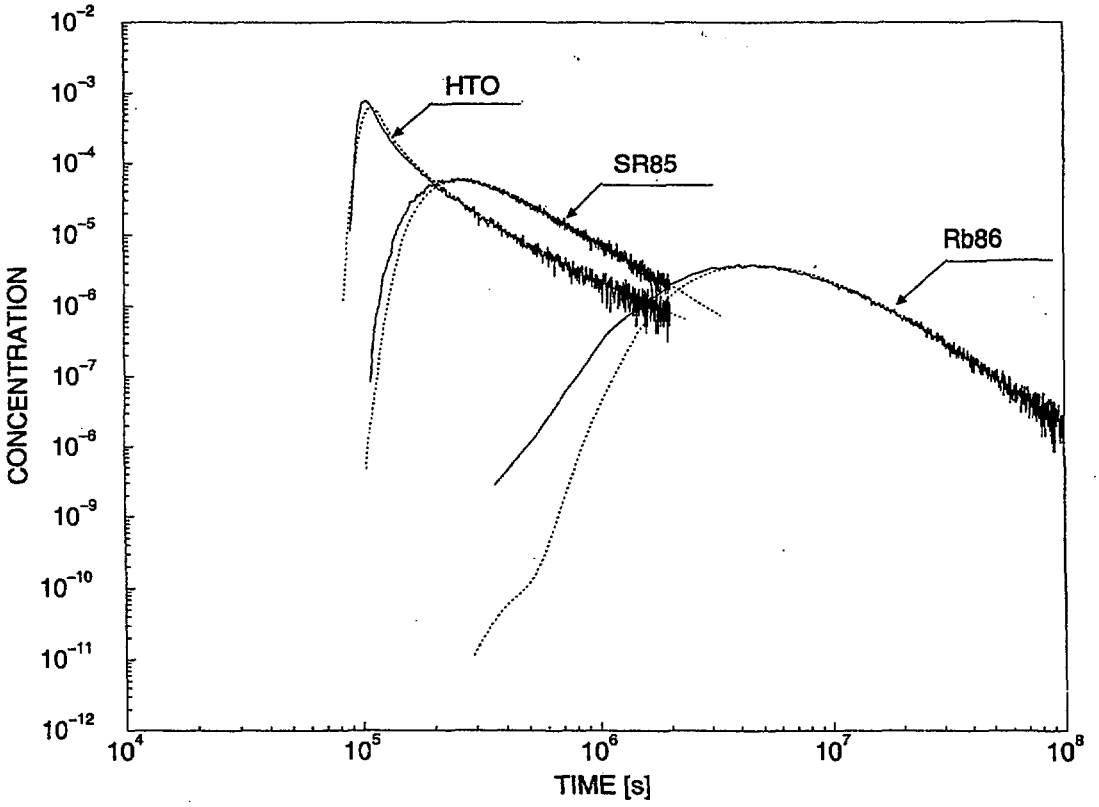


***Figure 4-11.*** *The multi-rate model. Comparison of breakthrough curves for HTO, SR85 and Rb86. Dotted lines give the results from the model by McKenna (1999).*

The comparisons presented are between two numerical models using different techniques to solve the same problem (McKenna uses advection-diffusion equations, while PARTRACK uses a particle tracking technique). It is of course encouraging that the two models give similar results, but there is also a further implication of the agreement. As McKenna (1999) has demonstrated that it is possible to model breakthrough curves from field experiments at Äspö with the multi-rate model, it is likely that also PARTRACK can be used to simulate these field experiments.

**Conclusion.** It has been verified that the implementation of the multi-rate model into PARTRACK is correct. Breakthrough curves for three tracers have been compared with the corresponding curves from the model by McKenna (1999). Good agreement is found except for early arrival times, which may be due to different concepts used for mechanical dispersion.

## 4.5 Simultaneously acting processes

**Description.** So far dispersion processes have been described one by one and, when possible, it has been verified that a process has been correctly implemented in PARTRACK. It is now time to demonstrate that all processes can act simultaneously in a three dimensional fracture network.

The simple fracture network shown in Figure 4-2 will be used, but now a third dimension will be added, see Figure 4-12. The first case considers advection with no dispersion and is hence similar, except for the dimensionality, to the test case described in Section 4.2.2. Then different dispersion processes (Taylor dispersion, channelling and multi-rate diffusion) will be added one by one and the modification of the breakthrough curve will be studied.

**Objective.** Demonstrate that PARTRACK can handle simultaneously acting dispersion processes in a three dimensional fracture network.

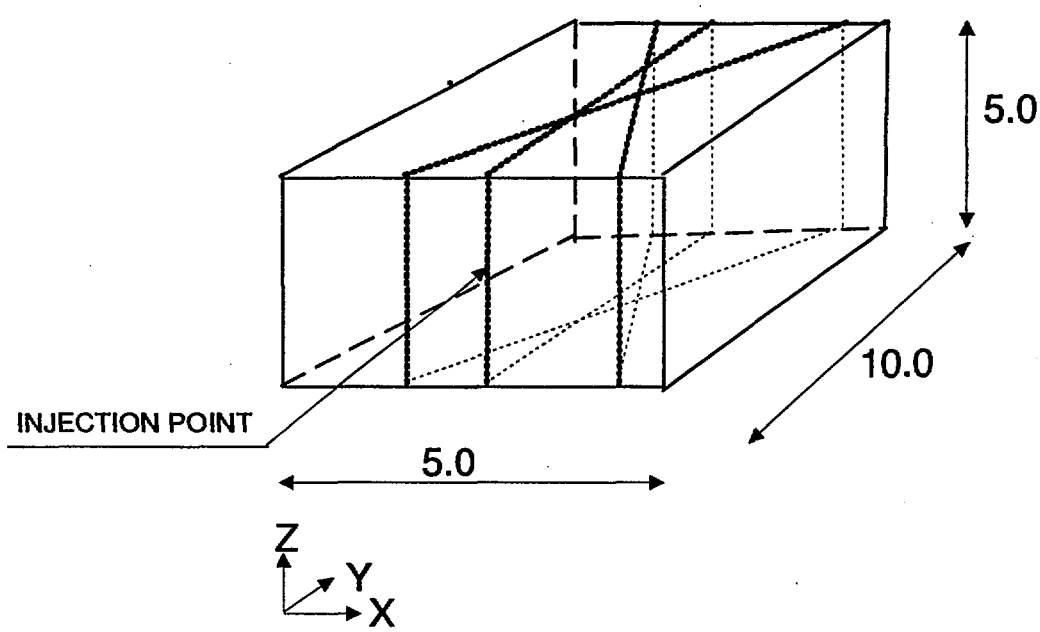


*Figure 4-12. Simultaneously acting processes. Outline of situation studied.*

**Results/Discussion.** As mentioned, the starting point is a fracture network in three dimensions. As no dispersion effects are considered, it is only the split up at fracture intersections that cause a broadening of the breakthrough curve. Dispersion processes, with the following characteristics, are then added one by one:

- Taylor dispersion with $D_m = 10^{-10}$ m$^2$/s.
- Variable aperture field. Isotropic correlation structure with correlation length = 0.3 m, $\overline{T} = 10^{-6}$ m$^2$/s, $\overline{e}_T = 10^{-3}$ m, $std(\log_{10} T) = 1.5$, $std(\log_{10} e_T) = 0.75$. All fractures have the same mean statistical properties.
- Multi-rate diffusion. Values for HTO, see Table 4-3, are used.

The resulting breakthrough curves can be studied in Figure 4-13. When no dispersion processes are activated (solid curve) it is possible to identify the peaks that are due to the different pathways. When Taylor dispersion is added these peaks are masked. A variable aperture field gives some additional dispersion due to the channelling effect. The multi-rate diffusion process adds a long tail to the breakthrough curve.

**Conclusion.** It has been demonstrated that PARTRACK can simulate all dispersion processes discussed simultaneously in a three dimensional fracture network.

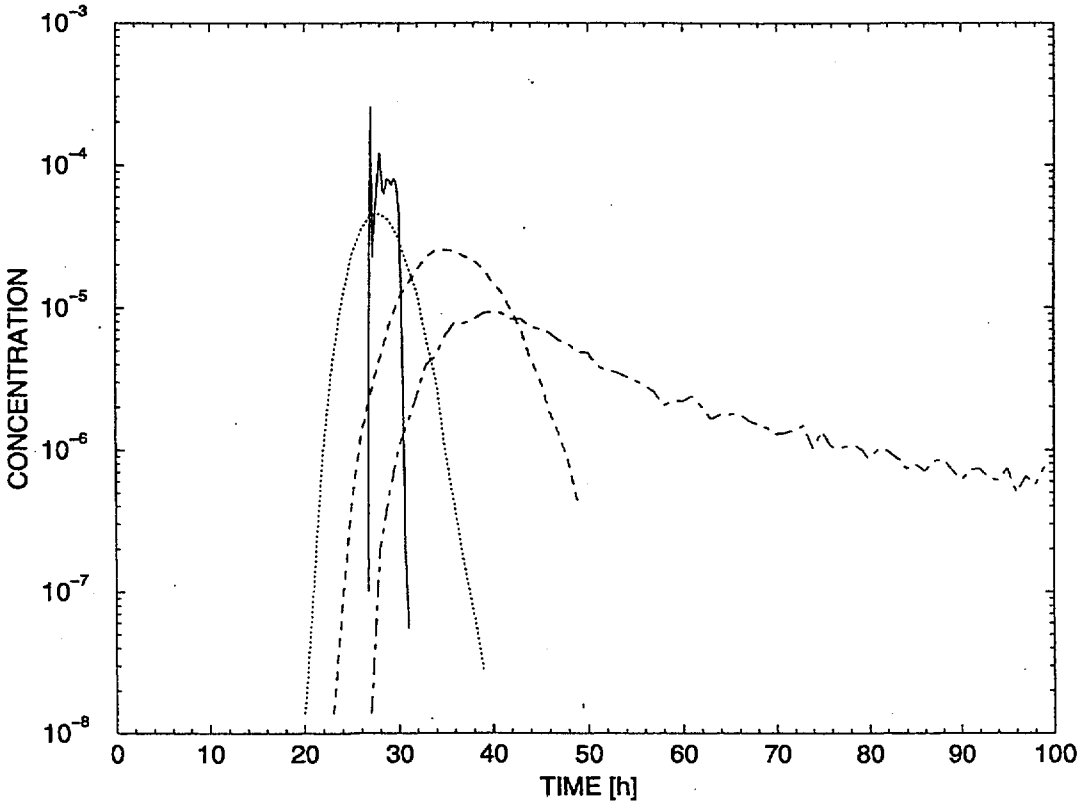


***Figure 4-13.*** *Simultaneously acting processes. Breakthrough curves.*
——— Advection only.
..... Taylor dispersion added.
------ Variable aperture added.
-·-·-· Multi-rate diffusion added.

# 5 Discussion and summary

From the previous section it is clear that PARTRACK can simulate many of the processes believed to be important for transport and dispersion of a solute in a sparsely fractured rock. It is then relevant to evaluate if PARTRACK is ready for, and suitable for, large scale real world applications. To facilitate this evaluation the key features, limitations and possible further developments of PARTRACK will be listed.

**Key features.** The capability and potential of PARTRACK is linked to a number of key features of the code:

- Full integration with the flow model presented in Svensson (1999a, b). In particular the conductivity field in the flow model is expected to be valuable for macro-dispersion. The flow model also calculates the kinematic porosity (Svensson, 2001), based on the porosity given for each fracture and fracture zone. PARTRACK also uses the same staggered grid arrangement as the flow model.

- PARTRACK is carefully verified by comparisons with analytical solutions and other codes (multi-rate diffusion model).

- PARTRACK can simulate Taylor dispersion in a correct and novel way (using the multiple particle states). Note that the classical way, using a longitudinal dispersion coefficient, may give transport upstream, i.e. against the flow (see de Marsily (1986), p. 242-243). The present method does not have this shortcoming.

- Dispersion due to channelling in a fracture or fracture zone can be simulated. An arbitrary number of fractures with their individual aperture correlation structure and orientation can be described in a three dimensional high resolution grid.

- PARTRACK is probably the first particle tracking model that can simulate Taylor dispersion, sorption and matrix diffusion simultaneously in a three dimensional flow field, as represented in a continuum model.

- It is effective in terms of computer time and storage. In many of the test cases presented 100 000 particles were used; the simulation time was on the order of a few minutes on a personal workstation.

**Limitations.** No major limitations have been identified so far. This may however change when field scale applications are attempted. Generally speaking, it is obvious that all uncertainties about input data (specification of the fracture network, porosities, boundary conditions, etc) will also cause an uncertainty in the transport simulations. This is however not related to the methods used in PARTRACK. Of similar nature is the necessity to introduce a grid and the assumptions related to the grid scale, $\Delta$. However, a genuine limitation of PARTRACK is that particles will not diffuse into a dead end fracture system as the particles will always "leave a cell with one of the outgoing flows". A dead end fracture system has no flow and will hence receive no particles. On the subgrid scale the multi-rate diffusion model will however simulate this effect.

**Further developments.** No further tests or developments are suggested at the present time. Instead it is suggested that PARTRACK should be applied to field scale situations. Comparisons with field experiments are of course of interest, but it may also be of value to make tests of a more generic nature, i.e. dispersion characteristics of a realistic fracture network.

# 6 Conclusion

It has, in the author's view, been demonstrated and verified that PARTRACK is an adequate framework for simulating transport and dispersion of a solute in a sparsely fracture rock. This statement is based on the results from an extensive range of test cases, which consider all major processes believed to be important for the problem.

# 7 Acknowledgement

The software package PARTRACK was written by Hans-Olof Kuylenstierna. His contribution has thus been of crucial importance to the project. The cooperation with Sean McKenna, Sandia National Laboratories, USA and his student Arun Waki in the comparison with the multi-rate model is acknowledged.

# 8 References

**Abelin H, Birgersson L, Moreno L, Widén H, Ågren T and Neretnieks I, 1991.** A large-scale flow and tracer experiment in granite 2. Result and interpretation. Water Resour. Res., vol. 27, no. 12, pp. 3119–3135.

**Bear J, Tsang C-F and de Marsily G, 1993.** Flow and contaminant transport in fractured rock. Academic Press, Inc.

**Cvetkovic V, Selroos J-O and Cheng H, 1999.** Transport of reactive tracers in rock fractures. J. Fluid Mech., vol. 378, pp. 335–356.

**de Marsily G, 1986.** Quantitative hydrogeology. Groundwater Hydrology for Engineers. Academic Press, Inc.

**Haggerty R and Gorelick S M, 1995.** Multiple-rate mass transfer for modelling diffusion and surface reactions in media with pore-scale heterogeneity. Water Resour. Res., 31 (19), pp 2383–2400.

**Haggerty R and Gorelick S M, 1998.** Modeling mass transfer processes in soil columns with pore-scale heterogeneity. Soil Sci. Soc. Am. J., 62 (1), pp. 62–74.

**Kuylenstierna H-O and Svensson U, 1994.** On the numerical generation of fracture aperture distributions. SKB Progress Report 25-94-18.

**McKenna S A, 1999.** Solute transport modelling of the Äspö STT-1b tracer tests with multiple rates of mass transfer. SKB International Cooperation Report ICR-99-02.

**Park Y-J and Lee K-K, 1999.** Analytical solutions for solute transfer characteristics at continuous fracture junctions. Water Resour. Res., vol 35, no 5, pp. 1531–1537.

**Rhén I (ed), Gustafson G, Stanfors R, Wikberg P, 1997.** Äspö HRL – Geoscientific evaluation 1997/5. Models based on site characterization 1986–1995. SKB Technical Report TR-97-06.

**Sahimi M, 1995.** Flow and transport in porous media and fractured rock. VCH Verlagsgesellschaft mbH, Weinheim.

**Spalding D B, 1981.** "A general purpose computer program for multi-dimensional one- and two-phase flow". Math. Comp. Sim., 8, 267–276. See also: http://www.cham.co.uk.

**Svensson U, 1992.** Modelling tracer transport in fractured porous media – An evaluation of concepts and methods using the LPT2 field experiment. SKB Progress Report 25-92-12.

**Svensson U, 1994.** Refined modelling of flow and transport in the numerical model of the Äspö Hard Rock Laboratory. SKB Progress Report 25-94-12.

**Svensson U, 1999a.** Representation of fracture networks as gridcell conductivities. SKB Technical Report TR-99-25.

**Svensson U, 1999b.** A laboratory scale analysis of groundwater flow and salinity distribution in the Äspö area. SKB Technical Report TR-99-24.

**Svensson U, 2001.** Representation of porosity and connectivity in a continuum model – Basic concepts, test cases and applications to the Äspö Hard Rock Laboratory. SKB draft Report.

# Documentation

**SKB – Äspö Hard Rock Laboratory**

Documentation of numerical simulation by Urban Svensson (US) 2000-08-15

**Object**

SKB purchase order no: 3203, 3548
Title of SKB purchase order: PARTRACK-Testcases, NUMMOD.
Author of report: US Company: CFE AB
Operator of computer and software: US Company: CFE AB

**Computer**

Name and version: Compaq/XP1000.

**Software**

Operative system: TRUE64 UNIX
Code name: PHOENICS 3.2 Main manual: On line
Program language: FORTRAN
Compiler: DIGITAL FORTRAN
Postprocessor name: Manual:
Postprocessor name: PHOTON Manual:
Subroutine: Report:
Subroutine: Report:
Subroutine: Report:

**Code verification**

Distributor: Not compiled in a single report.
Report/article:
Report/article:

**Other verification**

Report/article: See Svensson (1999a), (1999b) and Svensson (2001), as referenced in this report.
Report/article:

**Input data**

Ref: Rhén et al. (1997), see reference list.
Ref:
Ref:
Ref:

| | | |
|---|---|---|
| Data file name: | Data of issue: | Stored at: |
| Data file name: | Data of issue: | Stored at: |
| Data file name: | Data of issue: | Stored at: |

**Results**

Report/article: All given in this report.
Report/article:

| | |
|---|---|
| Data file name: | Stored at: |
| Data file name: | Stored at: |

**Condensed description of groundwater flow model.**

| A particle tracking algorithm for transport and dispersion of solutes in a sparsely fractured rock | |
|---|---|
| **Scope**<br>Verification and demonstration | |
| **Process description**<br>Conservation of mass, volume and momentum (Darcy's law).<br>Tracking of particles | |
| **Concepts** | **Data** |
| **Geometric framework and parameters** | |
| Domain divided into computational cells to which conservation laws are applied. | Domain size: varies<br>Computational grid: variable number of cells |
| **Material properties** | |
| Transmissivities.<br>Aperture.<br>Porosity | Data from Rhén et al. (1997). |
| **Spatial assignment method** | |
| Cell conductivities are calculated from a fracture network.<br>Porosity related to transmissivity | No field data is used. |
| **Boundary conditions** | |
| Zero flux or prescribed pressure. | No field data is used. |
| **Numerical tool**<br>PHOENICS | |
| **Output parameters**<br>Flux, pressure, particle tracks and positions. | |